An HIV-1 transgenic rat that develops HIV-related pathology and immunologic dysfunction

W. Reid*†, M. Sadowska†, F. Denaro*, S. Rao‡, J. Foulke, Jr.†, N. Hayes*, O. Jones*, D. Doodnauth*, H. Davis*, A. Sill§, P. O'Driscoll§, D. Huso¶, T. Fouts‖, G. Lewis‖**, M. Hill‖, R. Kamin-Lewis‖**, C. Wei††, P. Ray‡‡, R. C. Gallo†, M. Reitz†**, and J. Bryant*§§

*Animal Model Division and Divisions of †Basic Science, ‖Vaccine Research, and §Epidemiology and Prevention, Institute of Human Virology, University of Maryland, Baltimore, MD 21201; ‡Division of Comparative Medicine and **Department of Microbiology and Immunology, University of Maryland, Baltimore, MD 21201; ††Division of Thoracic and Cardiovascular Surgery, School of Medicine, University of Maryland, Baltimore, MD 21201; ‡‡Children's Research Institute, Children's National Medical Center, Washington, DC 20010; and ¶Division of Comparative Medicine, Johns Hopkins University School of Medicine, Baltimore, MD 21205

Contributed by R. C. Gallo, June 11, 2001

We report, to our knowledge, the first HIV type 1 (HIV-1) transgenic (Tg) rat. Expression of the transgene, consisting of an HIV-1 provirus with a functional deletion of *gag* and *pol*, is regulated by the viral long terminal repeat. Spliced and unspliced viral transcripts were expressed in lymph nodes, thymus, liver, kidney, and spleen, suggesting that Tat and Rev are functional. Viral proteins were identified in spleen tissue sections by immunohistochemistry and gp120 was present in splenic macrophages, T and B cells, and in serum. Clinical signs included wasting, mild to severe skin lesions, opaque cataracts, neurological signs, and respiratory difficulty. Histopathology included a selective loss of splenocytes within the periarterial lymphoid sheath, increased apoptosis of endothelial cells and splenocytes, follicular hyperplasia of the spleen, lymphocyte depletion of mesenteric lymph nodes, interstitial pneumonia, psoriatic skin lesions, and neurological, cardiac, and renal pathologies. Immunologically, delayed-type hypersensitivity response to keyhole limpet hemocyanin was diminished. By contrast, Ab titers and proliferative response to recall antigen (keyhole limpet hemocyanin) were normal. The HIV-1 Tg rat thus has many similarities to humans infected with HIV-1 in expression of viral genes, immune-response alterations, and pathologies resulting from infection. The HIV-1 Tg rat may provide a valuable model for some of the pathogenic manifestations of chronic HIV-1 diseases and could be useful in testing therapeutic regimens targeted to stages of viral replication subsequent to proviral integration.

HIV type 1 (HIV-1) infection is marked by a constellation of pathologies in addition to a variety of secondary infections (1). These include central and peripheral neuropathies (2), follicular lymph node hyperplasia (particularly early in infection; ref. 3), lymphoid depletion (at least in part involving apoptosis; refs. 4 and 5), interstitial pneumonitis (especially in pediatric cases; refs. 6 and 7), tubulointerstitial nephritis, glomerulosclerosis (8–10), wasting (11), and heart disease (12).

To establish a small-animal model for HIV-associated pathologies, several HIV transgenic (Tg) mice have been established. A *Tat* transgene was reported to cause dermal lesions resembling Kaposi sarcoma (13) or lymphoid hyperplasia in spleen and lymph nodes, and B cell lymphoma (14) when expression was regulated by the viral long terminal repeat (LTR) or a heterologous promoter, respectively. Expression of a *nef* transgene driven by the HIV-1 LTR also resulted in dermal lesions (15). More recently, Tg mice expressing *nef* under the control of a human T cell-specific promoter and mouse enhancer developed immunodeficiency with loss of T cells and alterations of T cell function (16). Tg mice also have been constructed with a *gag-pol*-deleted HIV-1 provirus regulated by the viral promoter and are characterized by wasting/runting, psoriatic skin lesions, cataracts, and nephropathy. Some HIV-1 gene expression occurs in most tissues, but is highest in skin and muscle (17, 18).

Despite replicating some of the pathologies in humans, viral expression in many existent HIV-1 Tg mouse models is regulated either by heterologous promoters, resulting in expression in atypical tissues, or by the viral promoter, which gives the highest expression in skin. The viral promoter does not function normally in mice, in part because mouse cyclin T does not interact functionally with Tat (19). We report here the construction of Tg rats that contain a *gag-pol*-deleted HIV-1 provirus regulated by the viral promoter. Unlike mice with the same transgene, efficient viral gene expression occurs in lymph nodes, spleen, thymus, and blood, suggesting a functional Tat. The Tg rat thus may offer significant advantages as a noninfectious small-animal model of HIV-1 pathogenesis.

Materials and Methods

Construction of HIV-1 *gag-pol*-Tg Rat. The construction of the plasmid from which the transgene was derived has been described (17). Briefly, a 3-kbp *Sph*I-*Msc*I fragment encompassing the 3′ region of *gag* and the 5′ region of *pol* was removed from pNL4–3, an infectious proviral plasmid, to make the noninfectious HIV-1$^{gag\text{-}pol}$ clone pEVd1443. A 7.4-kbp *Eae*I-*Nae*I fragment containing the provirus and host cell flanking regions was microinjected into fertilized one-cell Sprague–Dawley × Fisher 344/NHsd F1 eggs as described (20). The experimental protocol was approved by the University of Maryland Biotechnology Institute Institutional Animal Care and Use Committee.

Macrophages and B and T Cell Isolation. Splenocytes were purified on Histopaque-1083 (Sigma), counted, divided into 3 aliquots of 1.5×10^7 cells, and stained with primary mAbs by standard procedure (21). Each aliquot was labeled for 45 min at room temperature with a 1:100 dilution of anti-rat mAbs ED1 (MCA341R; Serotec), CD45RA (MCA340R; Serotec), or CD3 (22011D; PharMingen), which are specific for rat macrophages and B and T cells, respectively. Cells (10^7) were magnetically labeled with 20 μl of magnetic activated cell sorting (MACS) rat anti-mouse IgG1 (471-02) or goat anti-mouse IgG (484-02) (Miltenyi Biotec, Auburn, CA) for 15 min at 6–12°C. The magnetically labeled cell suspensions were separated by positive selection on MS+ separation columns placed in a VarioMACS magnet (Miltenyi Biotec), using the manufacturer's recommendations.

Abbreviations: DTH, delayed type hypersensitivity; H&E, hematoxylin and eosin; HIV-1, HIV type 1; KLH, keyhole limpet hemocyanin; PALS, periarterial lymphatic sheath; Tg, transgenic; LTR, long terminal repeat; Th, T helper.

§§To whom reprint requests should be addressed at: Animal Model Division, Institute of Human Virology, 725 West Lombard Street, Baltimore, MD 21201-1192. E-mail: bryant@umbi.umd.edu.

The publication costs of this article were defrayed in part by page charge payment. This article must therefore be hereby marked "*advertisement*" in accordance with 18 U.S.C. §1734 solely to indicate this fact.

Histology, Immunochemistry, and Apoptosis. Tissues from Tg and non-Tg littermates and Fisher 344/NHsd Sprague–Dawley control rats were fixed in 10% neutral buffered formalin and embedded in paraffin. Five-microgram tissue sections were used for hematoxylin and eosin (H&E) staining, immunohistochemistry, and apoptosis assays. A modified avidin/biotin method was used for immunohistochemical localization of HIV gene products (22). Paraffin sections were processed as described, exposed to antigen unmasking solution (Vector Laboratories), incubated in 3% H_2O_2 for 20 min, and treated with avidin/biotin blocking solution (Vector Laboratories) and nonimmune sera appropriate for blocking the secondary Ab at a 1:5 dilution. Primary Abs (all from Advanced Biotechnologies, Columbia, MD, except where noted) included HIV-1 gp120 goat antiserum (13-202-000), diluted 1:50 and 1:100; HIV-1 rabbit anti-HIV gp120 antiserum (13-204-000), diluted 1:100; mouse anti-HIV-1 gp120 mAb (NEN, Boston, MA; NEA 9301), diluted 1:150; mouse anti-HIV-1 Tat mAb (13-162-100), diluted 1:50 and 1:100; and mouse anti-HIV-1 Nef (13-152-1000), diluted 1:50 and 1:100. Biotinylated secondary Abs were incubated for 2 h at room temperature with anti-mouse IgG (rat-absorbed), anti-rabbit IgG, and anti-goat IgG (Vector Laboratories), at dilutions of 1:200–500, and labeled with Vecta Stain Elite ABC kit (Vector Laboratories), followed by addition of 3,3′-diaminobenzidine tetrahydrochloride (DAB) peroxidase (Sigma) or the 3-amino-9-ethylcarbazole (AEC) substrate system (Dako) to visualize the immunolabel.

Immunization of Rats. Tg and Fisher 344/NHsd control rats were immunized i.p. with 100 μg of keyhole limpet hemocyanin (KLH; Pierce) with complete Freund's adjuvant (Difco). Four weeks later, sera were collected, and anti-KLH end-point titers were determined by ELISA. Microtiter plates (NUNC MaxiSorp, Roskilde, Denmark) were coated with 2 μg/ml KLH overnight at 4°C. Plates were washed, blocked with 5% milk powder, and incubated with serially diluted rat sera at 37°C for 2 h. Bound IgG was detected with horseradish peroxidase-conjugated anti-rat IgG Ab. For detection of delayed type hypersensitivity (DTH), rats were challenged intracutaneously 4 weeks after immunization with 50 μg of KLH, and the size of the induration was measured 24 h later.

Proliferation Assays. Splenocytes (2.0×10^5) were cultured in 0.2 ml of RPMI medium 1640 with 10% (vol/vol) FBS in a microtiter plate with 50 μg/ml of KLH or 10 μg/ml of phytohemagglutinin. The cells were pulsed with 1 μCi of [^{3}H]thymidine (6.7 Ci/mmol; NEN) for 18–24 h and harvested onto glass fiber filters with a Micron 96-cell harvester (Skatron, Lier, Norway). Incorporation of [^{3}H]thymidine was measured with a liquid scintillation counter. All experiments were in triplicate.

Statistics. The mean number of apoptotic splenocytes per high power field, DTH measurements, and KLH end-point titers between phytohemagglutinin-stimulated and unstimulated cells from Tg and normal offspring were compared by using an independent Student's t test for samples exhibiting normally distributed values. A Wilcoxon rank sum test was used for samples exhibiting non-normal distribution. Two-tailed P values were considered significant at $P < 0.05$.

Results

Preliminary Analysis of HIV-1 Tg Rats. One female founder was produced that had very opaque cataracts. Mating with a wild-type Fischer 344/NHsd produced several F1 Tg and normal offspring. F1 offspring had very opaque (line 1) or very mild cataracts (line 2). The Tg animals were grouped according to cataract phenotypes, and DNA was prepared from tail tips, digested with *Eco*RI, and analyzed by Southern blotting (ref. 23;

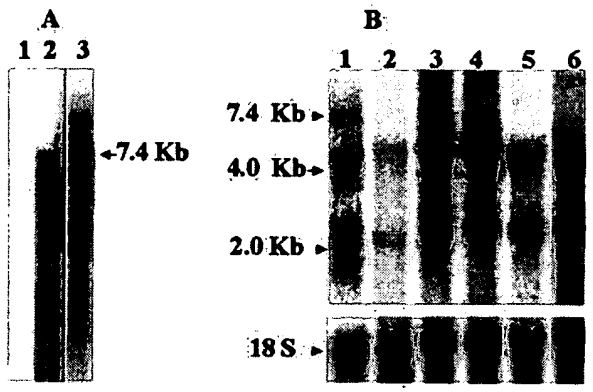

Fig. 1. Detection and expression of transgene. (*A*) Detection of transgene. A Southern blot was performed on *Eco*RI-digested DNA from tail snips of a normal rat (15 μg; lane 1) or Tg rats with mild (20 μg; lane 2) or very opaque (5 μg; lane 3) cataracts. The blot was hybridized to an α-^{32}P-labeled 7.4-kb *Eael-Nael* fragment from pEVd1443. (*B*) Expression of transgene RNA. A Northern blot was performed on total RNA isolate from various tissues and analyzed by Northern blot as described (32). HIV-specific transcripts (7-, 4-, and 2-kb) were detected with an α-^{32}P-labeled 1.3-kbp (*BglII/BglII*) fragment from pHXB2, containing gp41 and *nef* coding regions. HIV transcripts were quantified with a Storm 840 PhosphorImager (Molecular Dynamics) and normalized for hybridization to 18S rRNA by using an appropriate probe. RNA was from the axillary (lane 1) and mesenteric (lane 2) lymph nodes, thymus (lane 3), liver (lane 4), kidney (lane 5), and spleen (lane 6) of transgenic rat with highly opaque cataracts. The positions of the 7.0-kb full-length mRNA, 4-kb singly spliced *env* mRNA, and 2-kb multiply spliced mRNA are indicated.

Fig. 1*A*). *Eco*RI cuts the transgene once. As shown in lanes 2 and 3 of Fig. 1*A*, the hybridization patterns of DNA representing the two phenotypes differed. Both gave bands corresponding to a full-length transgene, as indicated by the arrow, suggesting that both integration sites contained two or more tandem copies of the transgene. Other bands, presumably representing transgene–host junction bands or head-to-tail multiple tandem integrated transgenes, differed, suggesting that the transgene had integrated at two independently segregating sites, one resulting in the opaque cataract phenotype and the other in mild cataracts. A brother–sister mating of F1 Tg rats from line 2 produced offspring with mild cataracts only. Southern blots of *Eco*RI-digested DNA from offspring were identical to those of the parents. As judged by the relative intensity of hybridization to Southern blots of Tg DNA compared with serial dilutions of known amounts of plasmid DNA quantified with a PhosphorImager (Molecular Dynamics), Tg rats from line 1 contained 20–25 copies, whereas those of line 2 contained only a few. Subsequent studies focused only on line 1 HIV-1 Tg rats.

HIV-1 Transgene Expression. RNA from numerous tissues was analyzed for viral transcripts. Expression levels were generally highest in lymph nodes, spleen, kidney, and thymus. A representative Northern blot of lymph node RNA (Fig. 1*B*) shows three viral-specific bands, representing full-length 7.4-kb mRNA, 4.0-kb singly spliced Env mRNA, and multiply spliced 2-kb mRNA transcripts for Nef, Tat, and Rev. The presence of Tat mRNA in the 2-kb band from spleen RNA was confirmed by reverse transcription–PCR amplification and DNA sequence analysis (not shown). Formalin-fixed paraffin-embedded 5-μm sections of spleen from line 1 (Fig. 1*B*) Tg rats were analyzed by immunohistochemistry for Env gp120, Nef, and Tat. All three proteins were evident in cells within the red and white pulp of the spleen (Fig. 2 *A–C*). Gp120 was present in cellular lysates of spleen-derived macrophages and B and T cells as judged by

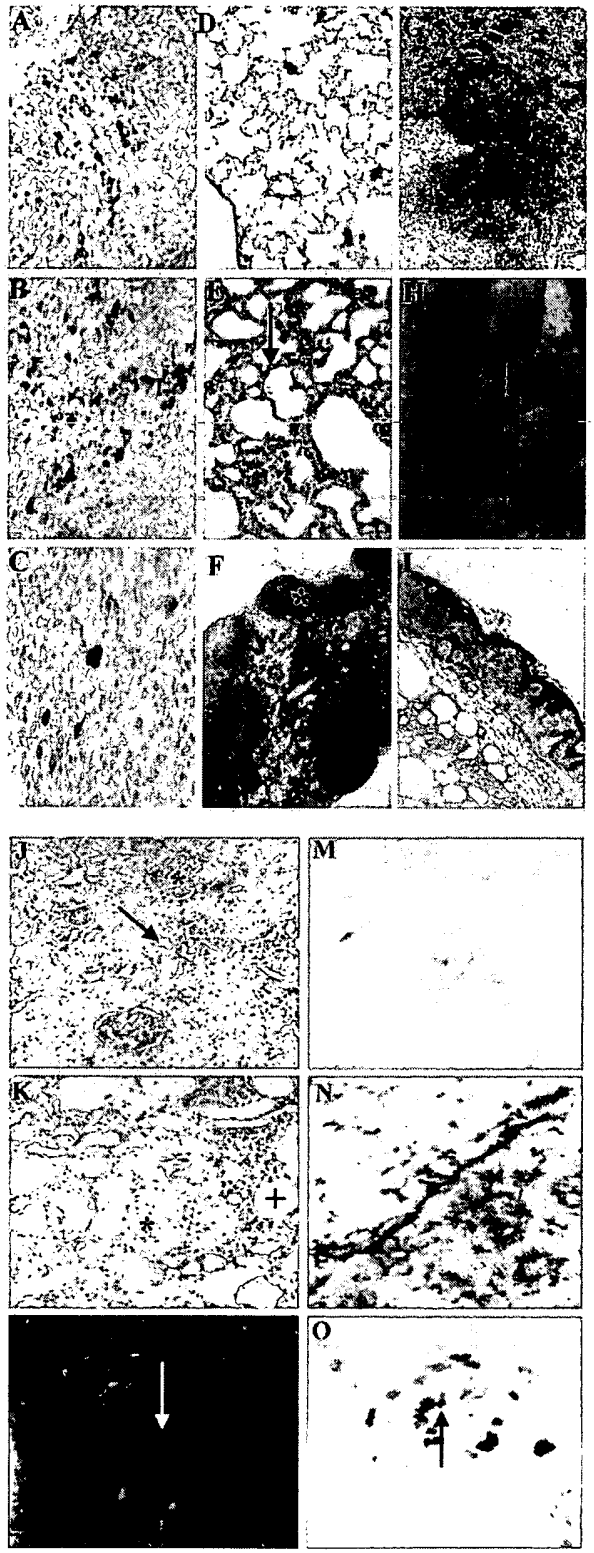

Fig. 2. Pathology and transgene expression. A section of Tg rat spleen was stained for HIV gp120 (*A*), Nef (*B*), and Tat (*C*). Cytoplasmic staining (dark brown) is evident for all three proteins (original magnification = ×60). H&E-stained sections of control (*D*) and Tg (*E*) lung are shown (×20). Arrow in *E* indicates area of interstitial thickening. H&E-stained sections of control (*F*) and Tg (*G*) mesenteric lymph node (×10) are shown. Note normal follicle (*, *F*) and hemorrhage, lymphoid depletion, and vascular proliferation in Tg section (*G*). Gross tail and foot lesions (*H*) and H&E-stained Tg skin (×60). Note psoriatic skin lesions with hyperkeratosis and mononuclear cell infiltrate (arrow, *I*). H&E-stained control kidney shows normal glomerulus (*) and renal tubule (arrow, *J*); Tg kidney shows focal glomerulosclerosis (*) and tubulointerstitial disease (+, *K*; ×60). H&E-stained heart section (*L*) shows myocardial inflammation with mononuclear cell infiltration (arrow) (×60). Astrocytes from normal (*M*) or Tg (*N*) brains were stained for glial fibrillary acidic protein (GFAP; ×40). Staining for GFAP was as reported (22), using anti-GFAP Ab (U7038; Dako). Staining of normal brain was limited, but Tg brain was heavily stained, indicating reactive gliosis, a marker for central nervous system damage. (*O*) Blood vessels in Tg brain were stained with ApopTag (×60); arrow indicates vascular endothelial apoptosis.

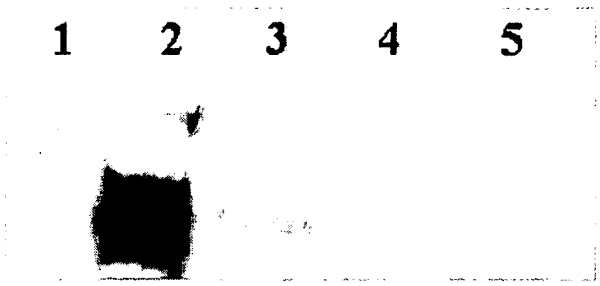

Fig. 3. Transgene expression in splenocytes. Seven micrograms of protein from extracts of spleen-derived macrophages (lane 3), B cells (lane 4), or T cells (lane 5) was fractionated on a 4–12% NuPage gel (NOVEX, San Diego) and analyzed by Western blot, using a 1:100 mouse anti-HIV-1 gp120 mAb (NEA 9301, NEN). Proteins were visualized by using the enhanced chemiluminescence (ECL) plus Western blotting system (Amersham Pharmacia). Lane 1 contained extract from a normal control spleen, and lane 2 contained 30 ng of recombinant gp120 as a positive control.

Western blotting (Fig. 3). The animals were also antigenemic. As measured by ELISA, sera contained 100–200 pg/ml of gp120 (Table 1). Thus, in marked contrast to Tg mice with the same proviral transgene (17, 18), Tg rats express viral gp120 in macrophages and B and T cells and shed it into peripheral blood.

Pathology of Tg Rats. Cataract formation ranged from mild to highly opaque. Some Tg animals (>50%) presented with highly angiogenic corneas. Their lenses had marked vacuolization, liquefaction, and fragmentation (not shown). In addition to cataracts, HIV-1 Tg rats developed many clinical manifestations of AIDS by 5–9 months of age, including weight loss, neurological abnormalities, and respiratory difficulty. Generally, neurological abnormalities were characterized by circling behavior and hind-limb paralysis. Often (>70%), the lung showed mild interstitial pneumonia characterized by mild to moderate interstitial fibrosis and mononuclear cell infiltration (Fig. 2 *D* and *E*). Mesenteric lymph nodes (>40%) were generally enlarged, and many histological sections showed lymphoid depletion and fibrosis (Fig. 2 *F* and *G*). Many Tg rats (>20%) had focal to extensive ulcerative skin lesions (Fig. 2 *H* and *I*). Histologically, the lesions were hyperkerototic, with elongation of the rete ridges. The kidneys from clinically ill rats (>90%) were diffusely pale, and the capsular surface was pitted, similar to what is seen with HIV-1 associated-nephropathy. H&E-stained kidney sections showed a spectrum of renal disease varying from mild to severe. Generally, glomeruli in Tg rats contained increased periodic acid/Schiff reagent (PAS)-positive material, with either segmental or global sclerosis. Some glomeruli showed mesangial hypercellularity and enlargement of visceral epithelial cells. Silver staining confirmed that the PAS-positive tissue within the

MEDICAL SCIENCES

Table 1. Serum gp120 in Tg rats

Tg rats	gp120, pg/ml*
Tg no. 1	151
Tg no. 2	129
Tg no. 3	121
Tg no. 4	85
Tg no. 5	172
Tg no. 7	235
Tg no. 8	164
Tg no. 9	217

The expression of gp120 envelope protein in the serum was assayed by ELISA antigen capture assay. The average gp120 concentration in the serum of hemizygous rats (n = 9) was 141 pg/ml (A).

*Capture ELISAs were done in triplicate on Tg rats with negative controls (n = 8). A mean adjusted value (76.6) for negative controls was subtracted.

glomeruli was composed of matrix material (not shown). The renal tubules showed microcystic tubular and tubulointerstitial pathology characterized by tubular degeneration, interstitial fibrosis, and mononuclear cell infiltration (Fig. 2 *J* and *K*). The heart generally was round and pale in color (not shown). Some hearts from Tg rats showed evidence of endocarditis and myocardial inflammation characterized by necrosis, mononuclear cell infiltrates, and multiple vascular abnormalities (Fig. 2*L*).

Tg rat brains with or without clinical neurological signs were grossly unremarkable. However, pathologic changes were evident in rats with clinical signs. Capillaries and endothelial cells presented with atypical changes, such as microscopic hemorrhages and endothelial cell apoptosis, in a multifocal distribution (Fig. 2*O*). Foci of gliosis together with neuronal cell death were noted, particularly in animals with clinically observable signs (Fig. 2*N*). For comparison, Fig. 2*M* shows a normal section of brain. Although the distribution of these changes seemed random, when they occurred with increased severity in focal areas of the brain, corresponding neurological deficits were noted. For example, animals with motor problems presented with greater severity of changes in the caudate putamen and substantia nigra.

Tg rat spleen was generally normal in size. Spleen tissue sections showed a loss of splenocytes within the periarterial lymphatic sheath (PALS), expansion of the marginal zones, follicular hyperplasia, and apoptosis of endothelial cells and splenocytes (Fig. 4 *A* and *B*). Apoptosis of splenocytes was evaluated by counting ApopTag (Intergen, Purchase NY)-positive cells per high-powered field in 5-month-old male rats and was significantly elevated compared with age- and sex-matched non-Tg controls ($P < 0.01$; Fig. 4*C*).

Immune Function of HIV-1 Tg Rats. To evaluate immune function, Tg rats and age-matched controls were immunized with KLH, and the resultant KLH-specific DTH responses and anti-KLH Ab titers were determined. The DTH response was determined from the extent of induration present at 24 h. The induration was significantly lower relative to controls ($P < 0.01$; Table 2). In contrast, there was no significant difference in anti-KLH-specific Ab titers, suggesting that the Tg rats have an abnormal T helper (Th)-1 response but normal Th2 function. The mean proliferative response of spleen cells from adult Tg rats to nonspecific mitogen (phytohemagglutinin) was significantly increased after 6 days compared with littermate controls ($P = 0.0062$; Table 3). However, there were no statistical differences in the T cell proliferative response of splenocytes from vaccinated rats to a recall antigen (KLH).

Discussion

We report, to our knowledge, the first HIV-1 Tg rat. The transgene, consisting of an HIV-1 provirus deleted for *gag* and

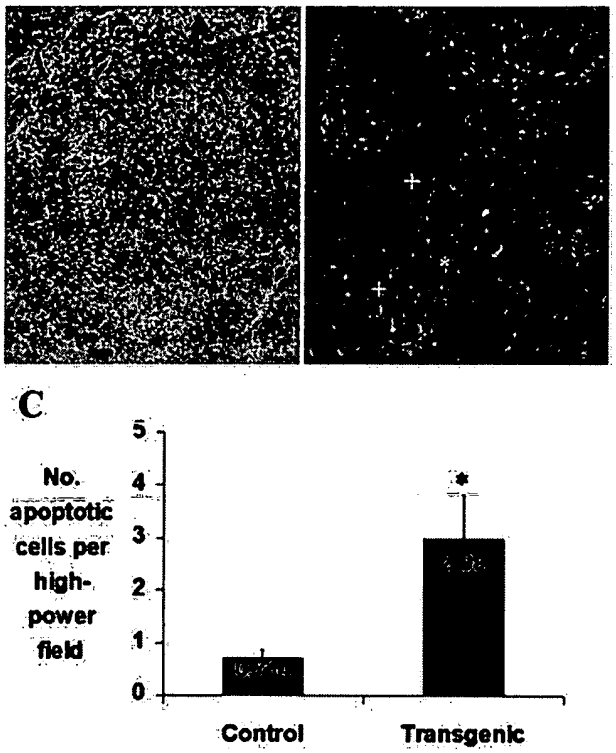

Fig. 4. Pathology and apoptosis in Tg rat spleen. (*A*) H&E-stained control spleen. Note T cell region (PALS) (*) and B cell region (marginal zone) (+) (original magnification ×60). (*B*) H&E-stained Tg rat spleen (×60). Note loss of T cells within the PALS (*). The two + show the marginal zone. (*C*) Five-microgram tissue sections were assayed *in situ* for apoptosis by using an ApopTag kit. Spleen sections from 5-month-old male Tg and Fisher 344/NHsd control rats were taken from 3 animals per group, and apoptotic cells from each section were enumerated 3 times at ×400 by using a Nikon Labophot-2 light microscope. The entire tissue section was counted by using a stage micrometer to pick successive nonoverlapping fields. The * shows the statistically significant difference between HIV-1 transgenic rats and age-matched controls.

pol, is expressed in lymphoid tissues, including lymph nodes, spleen, thymus, and blood. The Tg rats exhibit pathologies and immune irregularities characteristic of HIV-1 infection of humans.

The tissue-specific pattern of viral gene expression is of interest. To model viral gene expression in infected humans, we

Table 2. Antibody and DTH responses to KLH in HIV-1 Tg rats

Exp. group	Observations	Anti-KLH Ab titer	Anti-KLH DTH, mm diameter	SE
Tg*	12	7.4	NA	0.19
Control*	6	7.9	NA	0
Tg†	10	NA	3.5‡	0.7
Control†	6	NA	10.8	1.4

NA, not applicable.

*Tg and non-Tg rats were immunized i.p. with 100 μg of KLH with complete Freund's adjuvant. Four weeks later, sera was collected, and end-point anti-KLH Ab titers were determined by ELISA. The results are expressed as mean ± SE (logarithm 10) of end-point titers.

†Immunized rats were challenged with 50 μg of KLH intracutaneously, and the size of the induration was measured 24 h later. Results are expressed as mean ± SE of diameter of induration (mm).

‡Indicates a statistical significance between HIV-1 Tg and non-Tg rats.

Table 3. Proliferative response of splenocytes from Tg

Exp. group	Observations	[^{3}H]thymidine incorporation of stimulated spleen cells, Δcpm		
		PHA	KLH	SE
Tg*	8	28,289‡	NA	7,201
Control*	5	2,138	NA	1,070
Tg†	4	NA	89,202	18,147
Control†	3	NA	92,475	24,260

NA, not applicable.

*Spleen cells (2×10^5) from HIV-1 Tg or non-Tg rats were cultured with 10 μg/ml of PHA at 37°C for 6 days.

†Spleen cells (2×10^5) from HIV-1 Tg or non-Tg rats immunized with KLH 4 weeks previously were cultured with 50 μg/ml KLH at 37°C for 5 days. All cells were labeled with 1 μCi [^{3}H]thymidine for the last 18–24 h, harvested, and the incorporated radioactivity counted. The results are expressed as mean ± SE of thymidine incorporation in triplicate cultures.

‡Indicates a statistical significance between Tg and non-Tg rats.

used the viral LTR to regulate the transgene. LTR-regulated gene expression depends on transactivation by the viral Tat protein, which requires cellular cyclin T as a cofactor. Mouse cyclin T is not functional with Tat, and LTR-driven expression in Tg mice differs from expression in humans, with the highest levels in skin and muscle. In contrast, viral genes are efficiently expressed in lymphoid tissues of Tg rats, similar to infected humans, suggesting that rat cyclin T is functional. A similar suggestion has been made by Bieniasz and Cullen (24). Three sizes of viral transcripts can be detected, including a 7.4-kb unspliced mRNA, a 4.3-kb singly spliced (*env*) mRNA, and a 2-kb multiply spliced (*tat*, *rev*, and *nef*) mRNA, similar to infected human cells, suggesting that Rev, a viral protein that regulates splicing, can also function in rats.

Clinical manifestations, similar to those in humans infected with HIV, are evident in the Tg rats, including neurological changes, respiratory difficulty, and cataracts. The neuropathology includes reactive gliosis, neuronal cell loss, lymphocyte infiltration, and alteration of endothelial cells with loss of blood–brain barrier integrity. There is a degeneration of peripheral nerves and skeletal muscle atrophy similar to that in infected humans. The Tg rat could be a useful model of HIV–central nervous system interactions, because the neuroanatomy, neurophysiology, neuropathology, and behavior of rats are well studied.

Pneumonitis associated with HIV-1 infection is common in pediatric cases of AIDS (6); however, its pathogenesis is not well understood. Most cases of pneumonia in people infected with HIV-1 are characterized by lymphocytic interstitial pneumonitis. Respiratory difficulty in the Tg rats is correlated with a mild expansion of the lung interstitium by a mononuclear infiltrate. The pneumonia in the Tg rats is unlikely to be caused by opportunistic infections, because of their pathogen-free status, sterile housing conditions, and certified diet, suggesting that pathogenesis is mediated directly by the HIV-1 transgene.

Cardiac disorders including myocarditis and cardiomyopathies have been reported in patients infected with HIV, but their etiopathogenesis is uncertain (12, 25, 26). The cardiac pathology seen in the Tg rats is grossly and microscopically similar to that in infected people, suggesting that this could be a useful model for the study of HIV-associated cardiac disease. There is controversy about the role of HIV as the primary etiology of cardiac pathology; opportunistic infections, cardiotoxic substances, nutritional deficiencies, and autoimmune reactions have been suggested as contributing factors. Because the Tg rats are pathogen-free, the observed cardiac abnormalities are likely caused by viral gene product activity rather than opportunistic infections.

Renal abnormalities are frequently seen in AIDS, especially in African-American patients (8, 27, 28). The most typical is HIV-1 associated-nephropathy (HIVAN), occurring in 10–15% of all infected African-American patients. HIVAN includes proteinuria, nephrotic syndrome, focal or segmental glomerulosclerosis, and tubulo-interstitial disease, rapidly progressing to end-stage renal disease. The pathogenesis is not completely understood but likely involves the direct effects of HIV-1 and cytokines such as basic fibroblast growth factor (bFGF) and transforming growth factor (TGF)-β (28) that are secreted by infected cells (29). The Tg rat offers a potential model for HIVAN and related conditions.

HIV-1 Tg rats have selective immune abnormalities. There is a markedly decreased DTH response but Ab titers and the proliferative response of splenocytes to KLH antigen is normal. Lymphoid tissues manifest an AIDS-like histopathology, including lymphocyte depletion in lymph nodes, severe splenic hyperplasia with loss of cells around the PALS, and increased apoptosis of splenocytes. Viral proteins are expressed in spleen T and B cells and monocytes. This hyperplasia and cell loss may be caused in part by abnormal trafficking of cells or by abnormal or selective proliferation and loss of lymphocyte subsets. It has recently been shown in mice that $CD8\alpha^+$ dendritic cells and naïve and Th1 T cells concentrate within the PALS, whereas $CD8\alpha^-$ dendritic cells and Th2 cells form loose rings around the outer PALS in close proximity to the B cells (30, 31). It is tempting to speculate that the loss of T cells around the PALS and in lymph nodes, the increased apoptosis in spleen, and the diminished DTH reaction are the results of a common mechanism affecting Th1 development or trafficking. Taken together with the pattern of pathologies that occur, the HIV-1 Tg rat is potentially a highly useful small-animal model for AIDS pathogenesis.

We thank the Institute of Human Virology ELISA Core Facility, Manhattan Charurat, Sayhed Abdel-Wahab, and Drs. David Hone, Simon Agwale, and Minglin Li for supporting this study. This research was supported in part by Public Health Service Grants 1K08 AI01792, NS 31857, and NS 39250, and by the Elisabeth Glaser Grant for Studies in Pediatric AIDS.

1. Popovic, M. & Gartner, S. (1989) *Curr. Opin. Immunol.* **1**, 516–520.
2. Price, R. W. (1996) *Lancet* **348**, 445–452.
3. Burke, A. P., Benson, W., Ribas, J. L., Anderson, D., Chu, W. S., Smialek, J. & Virmani, R. (1993) *Am. J. Pathol.* **142**, 1701–1713.
4. Gallo, R. C. & Montagnier, L. (1988) *Sci. Am.* **259**, 41–48.
5. Fauci, A. S. (1993) *Eur. J. Immunol.* **262**, 1011–1018.
6. McSherry, G. D., Mootsikapun, P., Chetchotisakd, P., Intarapoka, B., Schneider, R. F. & Rosen, M. J. (1996) *Semin. Respir. Infect.* **11**, 173–183.
7. Mootsikapun, P., Chetchotisakd, P. & Intarapoka, B. (1996) *J. Med. Assoc. Thai* **79**, 477–485.
8. Bourgoignie, J. J., Glassock, R. J., Cohen, A. H., Danovitch, G. & Parsa, K. P. (1989) *Klin. Wochenschr.* **67**, 889–894.
9. Seney, F. D., Jr., Burns, D. K., Silva, F. G., Bourgoignie, J. J., Glassock, R. J., Cohen, A. H., Danovitch, G. & Parsa, K. P. (1990) *Am. J. Kidney Dis.* **16**, 1–13.
10. Klotman, P. E. (1999) *Kidney Int.* **56**, 1161–1176.
11. Strawford, A. & Hellerstein, M. (1998) *Semin. Oncol.* **25**, 76–81.
12. Patel, R. C. & Frishman, W. H. (1996) *Med. Clin. N. Am.* **80**, 1493–1512.
13. Vogel, J., Hinrichs, S. H., Reynolds, R. K., Luciw, P. A. & Jay, G. (1988) *Nature (London)* **335**, 606–611.
14. Vellutini, C., Horschowski, N., Philippon, V., Gambarelli, D., Nave, K. A. & Filippi, P. (1995) *AIDS Res. Hum. Retroviruses* **11**, 21–29.
15. Dickie, P., Ramsdell, F., Notkins, A. L. & Venkatesan, S. (1993) *Virology* **197**, 431–438.
16. Hanna, Z., Kay, D. G., Rebai, N., Guimond, A., Jothy, S. & Jolicoeur, P. (1998) *Cell* **95**, 163–175.
17. Dickie, P., Felser, J., Eckhaus, M., Bryant, J., Silver, J., Marinos, N. & Notkins, A. L. (1991) *Virology* **185**, 109–119.
18. Santoro, T. J., Bryant, J. L., Pellicoro, J., Klotman, M. E., Kopp, J. B., Bruggeman, L. A., Franks, R. R., Notkins, A. L. & Klotman, P. E. (1994) *Virology* **201**, 147–151.

19. Wei, P., Garber, M. E., Fang, S. M., Fischer, W. H. & Jones, K. A. (1998) *Cell* **92**, 451–462.
20. Lacy, E., Costantini, F., Beddington, R. & Hogan, B., eds. (1994) *Manipulating the Mouse Embryo* (Cold Spring Harbor Lab. Press, Plainview, NY).
21. Coligan, J. E., Kruisbeek, A. M., Margulies, D. H., Shevach, E. M. & Strober, W., eds. (1994) *Current Protocols in Immunology* (Wiley, New York).
22. Wiley, C. A., Schrier, R. D., Denaro, F. J., Nelson, J. A., Lampert, P. W. & Oldstone, M. B. (1986) *J. Neuropathol. Exp. Neurol.* **45**, 127–139.
23. Southern, E. M. (1975) *J. Mol. Biol.* **98**, 503–517.
24. Bieniasz, P. D. & Cullen, B. R. (2000) *J. Virol.* **74**, 9868–9877.
25. Barbaro, G., Di Lorenzo, G., Grisorio, B. & Barbarini, G. (1998) *AIDS Res. Hum. Retroviruses* **14**, 1071–1077.
26. Guillamon, T. L., Romeu, F. J., Forcada Sainz, J. M., Curos, A. A., Larrousse, P. E. & Valle, T. V. (1997) *Rev. Esp. Cardiol.* **50**, 721–728.
27. Bourgoignie, J. J., Ortiz-Interian, C., Green, D. F. & Roth, D. (1989) *Transplant. Proc.* **21**, 3899–3901.
28. Ray, P. E., Liu, X. H., Xu, L. & Rakusan, T. (1999) *Pediatr. Nephrol.* **13**, 586–593.
29. Liu, X. H., Hadley, T. J., Xu, L., Peiper, S. C. & Ray, P. E. (1999) *Kidney Int.* **55**, 1491–1500.
30. Randolph, D. A., Huang, G., Carruthers, C. J., Bromley, L. E. & Chaplin, D. D. (1999) *Eur. J. Immunol.* **286**, 2159–2162.
31. Moser, M. & Murphy, K. M. (2000) *Nat. Immunol.* **1**, 199–205.
32. Puissant, C. & Houdebine, L. M. (1990) *BioTechniques* **8**, 148–149.